Letters

Four Quadrants Integrated Transformers for Dual-Input Isolated DC–DC Converters

Ziwei Ouyang, Zhe Zhang, Michael A. E. Andersen, and Ole C. Thomsen

***Abstract*—A common limitation of power coupling effect in some known multiple-input dc–dc converters has been addressed in many literatures. In order to overcome this limitation, a new concept for decoupling the primary windings in the integrated multiple-winding transformers based on 3-D space orthogonal flux is proposed in this letter. And thus, a new geometry core and relative winding arrangements are proposed in accordance with the orthogonal flux decoupling technology. Due to the four secondary windings are arranged in a quadratic pattern at the base core plate with the two perpendicular primary windings, a name of "four quadrants integrated transformers" (FQIT) is, therefore, given to the proposed construction. Since the two primary windings are uncoupled, the FQIT allows the two input power stages to transfer the energy into the output load simultaneously or at any time-multiplexing scheme, which can optimize the utilization of input sources, simplify the system structure, and reduce the overall cost, so they are attractive for the hybrid renewable power system. Section IV initiates a discussion for the advantages of the FQIT. In order to verify the feasibility of the FQIT in multiple-input converter, a dual-input isolated boost dc–dc converter with the FQIT is designed and tested. The results have excellently demonstrated that the two input power stages can be operated independently and the correctness of all the analysis in the letter.**

***Index Terms*—DC-DC, decoupling, integrated transformer, multiple-input converter (MIC), phase shift.**

I. Introduction

MULTIPLE-INPUT converters (MICs) have been proposed as a cost-effective and flexible way to interface various sources such as solar array, wind turbine, fuel cell, and commercial ac line, to get a regulated output voltage, and in some cases, energy-storage devices, with a load [1]–[4]. A common limitation of some known MICs is that only one input power source is allowed to transfer the power energy to the output at a time to prevent power coupling effect. Recently, in order to overcome this limitation, it has been proposed to use multiple-winding transformers based on flux additivity technology with phase-shifted pulsewidth modulation (PWM) control [5]. This technology can transfer power from two or multiple different input voltage sources to the output load simultaneously meanwhile reverse blocking diodes are required at the input power stage sides. The reverse blocking diodes are needed to prevent a reverse power flow from one of the input voltage sources to another input voltage source through the coupled primary sides of the transformer as well as body diodes of semiconductor switches of the input power stages. Without these reverse blocking diodes, different input sources coupled to the multiple-input power converter cannot deliver power to the load simultaneously. Furthermore, this technology cannot be applied in the buck type isolated MICs unless the input voltages are strictly limited according to the turns ratio of multiple primary windings. Otherwise, an undesirable voltage difference stresses on one of the input power stages, causing an extremely high current on the semiconductors and, thus, damages the circuit. In addition, some other prior art approaches nowadays to overcome this limitation result in a large number of power switches and complicated control schemes [6], [7].

The main reason for the problem in the MICs is that the multiple primary windings are coupled. Consequently, it would be advantage to provide an integrated transformer with uncoupled primary windings for use in the MICs to allow multiple input power sources to be operated independently without compromising any functions of the power converter or required complex control or protection circuitry to be added to the input power stages. However, the existing decoupling approaches applied to the traditional core geometries such as E-I or E-E rely on a shared lower reluctance path or flux cancellation mechanisms [8]. In practical, both approaches applied to the traditional cores will cause lower magnetizing inductances, higher winding loss, and EMI problem [9]–[11]. Hereby, this letter proposes a new flux decoupling concept for the multiple-winding transformers used in the MICs. As shown in Fig. 1(a), the new flux decoupling concept is based on 3-D space orthogonal flux decoupling wherein the three flux paths extend substantially orthogonally to each other within the shared magnetically permeable core. This requires a sort of nontraditional core geometries to carry out the orthogonal flux paths, shown in Fig. 1(b). Since this letter focuses on a new idea and its specific contributions rather than a detailed circuit analysis for its applicable topologies, the construction of this letter is accordingly organized as follows.

Manuscript received October 3, 2011; revised December 12, 2011; accepted January 26, 2012. Date of current version March 16, 2012. This work was supported by Flux A/S and has been filed as EU and U.S. patent. Recommended for publication by Associate Editor B. Choi.

The authors are with the Department of Electrical Engineering, Technical University of Denmark, Kgs. Lyngby DK-2800, Denmark (e-mail: zo@elektro.dtu.dk; zz@elektro.dtu.dk; ma@elektro.dtu.dk; oct@elektro.dtu.dk).

Color versions of one or more of the figures in this paper are available online at http://ieeexplore.ieee.org.

Digital Object Identifier 10.1109/TPEL.2012.2186591

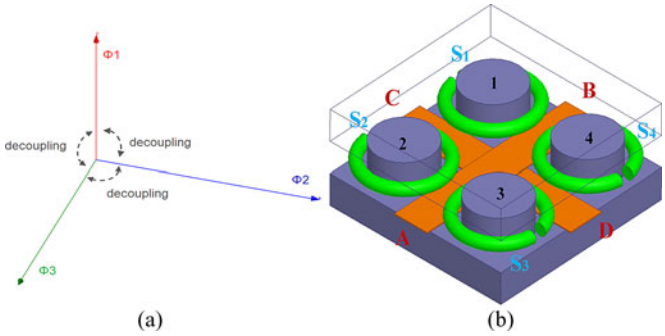

Fig. 1. (a) 3-D space orthogonal flux decoupling. (b) Proposed integrated transformer with four quadrants structure.

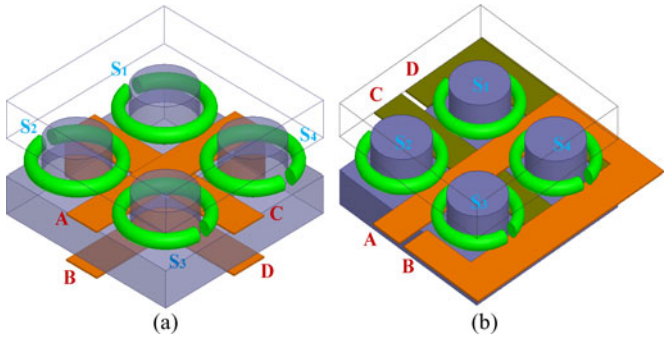

Fig. 2. Available structures for plurality turns of (a) vertical directed (b) horizontal directed primary windings.

Section II briefly presents the modeling of the proposed four quadrants integrated transformer (FQIT). Section III describes an operational principle of the FQIT used in dual-input isolated boost dc–dc converter. Section IV initiates a discussion of the advantages of the proposed transformer. In order to verify the feasibility of the proposed transformer and the correctness of its analysis, an experimental dual-input isolated boost dc–dc converter employed with the proposed integrated transformer has been built. The experimental results are shown in Section V.

II. Modeling of FQIT

As shown in Fig. 1(b), the magnetically permeable core comprises a base rectangular core plate with four legs situated at respective corners, and a top rectangular core plates. In order to clearly illustrate the winding arrangements, a transparent top-core plate is drawn in Fig. 1(b). The first primary winding *AB* and the second primary winding *CD* are orthogonally arranged as a cross-shaped layout in-between the four legs. By using the right-hand rule, the flux generated from winding *AB* is substantially orthogonal to the flux generated from winding *CD* in the base and top-core plates, and thus the uncoupled primary windings are constructed. The four legs provide a shared magnetic flux path to the two primary windings where the four secondary windings, S_1, S_2, S_3, and S_4, are wound in each, respectively. Therefore, the two primary windings are both coupled with the four secondary windings. A name of FQIT is given to the proposed integrated transformer since the four legs with enclosed secondary windings are arranged in a quadratic pattern at the base core plate with the two perpendicular primary windings. The plurality turns of primary windings can be arranged as shown in Fig. 2(a) and (b).

III. Operation Principle of FQIT

This transformer can be used in many different topologies employing the multiple-winding transformers. In order to describe a basic principle of the FQIT, a dual-input isolated boost dc–dc converter is given in Fig. 3 as an example. In the secondary side, the windings wound in the diagonal legs, S_1 and S_3, S_2 and S_4 are connected in series with a reverse coupled winding direction. The respective series-wound are electrically coupled to their individual rectifiers and then in parallel connected to the output load.

The direction and amplitude of the magnetic fluxes in the legs are dependent on the magnetizing currents of the primary windings. Accordingly, the four stages of the magnetic fluxes through the legs in accordance with the magnetizing current states have been depicted in Fig. 4. The directions for the magnetizing currents of the primary windings, i_{T1} and i_{T2}, are indicated by solid arrows. The corresponding magnetic fluxes through the four legs induced by the two currents are indicated by the dash arrows, respectively. Due to the full-bridge boost converter, the duty cycle must be operated above 50% to ensure switch overlap, and thus, a continuous current path for the boost inductor current. Accordingly, typical primary voltage waveforms V_{T1} and V_{T2} with zero voltage platforms are produced as depicted in Fig. 5 and a 75% duty cycle is given as an example.

1) Stage 1 (t_0–t_1): The magnetizing current i_{T1} is positive and the magnetizing current i_{T2} is negative. This current state is characterized by the indicated direction shown in Fig. 4(a). Using the right-hand rule, the current i_{T1} leads to the magnetic fluxes in the leg 1 and leg 2 (Leg 1 is the leg corresponding with the winding S_1. The rest may be deduced by analogy.) flowing along the same direction indicated by the yellow dash arrows. This is a consequence of the leg 1 and the leg 2 being arranged on the same side of the primary winding AB. Furthermore, the current i_{T1} also leads to the magnetic fluxes in the leg 3 and leg 4 flowing along the same direction. The magnetic fluxes induced by the current i_{T1} leads to oppositely directed fluxes in the leg 1 and leg 2 relative to the leg 3 and leg 4 which is a consequence of the geometry of the closed magnetic flux loop. Likewise, the current i_{T2} leads to the same flux directions in the leg 1 and leg 4 indicated by the blue dash arrows. The opposite flux direction relative to the flux direction in the leg 1 and leg 4 are induced in the leg 2 and leg 3 by the current i_{T2}. Hereby, a flux cancellation can be observed in the leg 1 and leg 3, meanwhile an overlapped flux occurs in the leg 2 and leg 4.

2) Stage 2 (t_1–t_2): The magnetizing currents i_{T1} and i_{T2} are both positive. This current state is characterized by the indicated direction shown in Fig. 4(b). The magnetic fluxes induced by the current i_{T1} through all four legs keep the same directions with those produced in the Stage 1 since the direction of the current

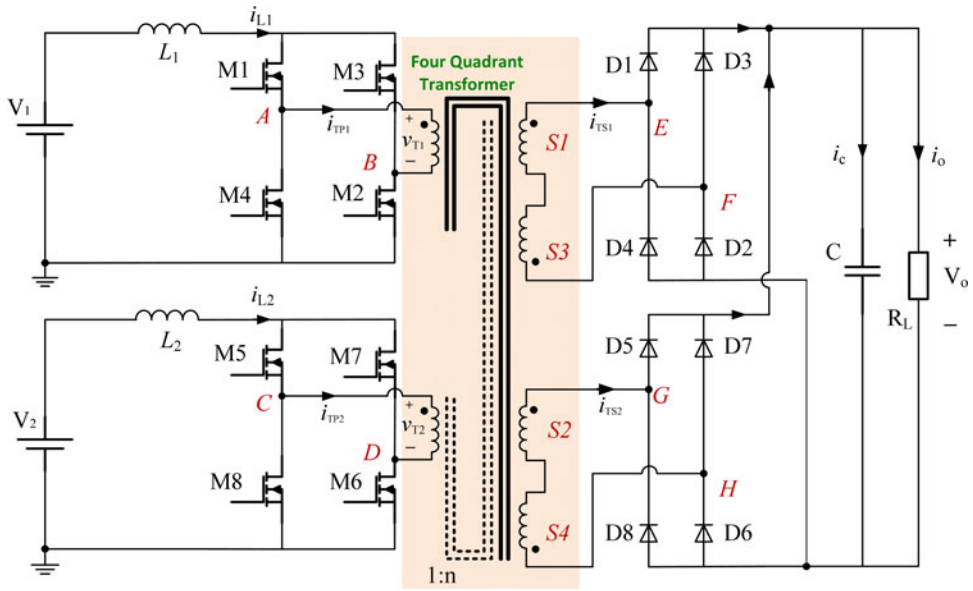

Fig. 3. Dual-input isolated boost dc–dc converter with FQIT.

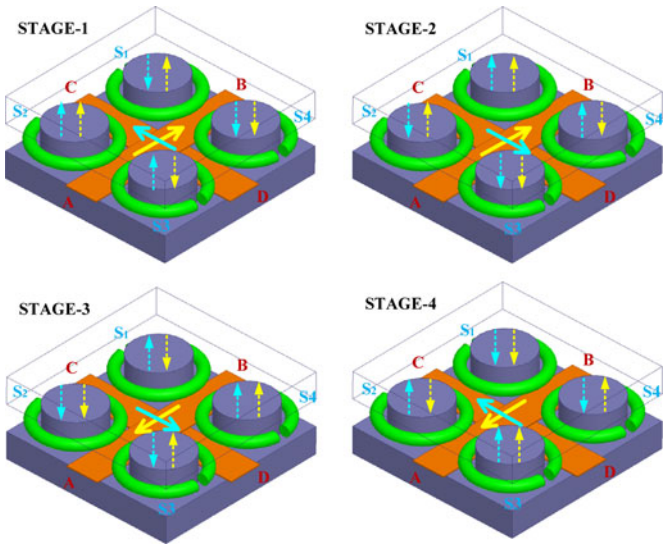

Fig. 4. Four stages of flux directions through the legs.

i_{T1} is not changed. However, as the direction of the current i_{T2} is changed, the directions of the induced magnetic fluxes indicated by the blue dash arrows are accordingly changed. Hereby, a flux cancellation can be observed in the leg 2 and leg 4, meanwhile an overlapped flux occurs in the leg 1 and leg 3.

3) Stage 3 (t_2–t_3): The magnetizing current i_{T1} becomes negative and the magnetizing current i_T2 still keeps positive. This current state is characterized by the indicated direction shown in Fig. 4(c). All magnetic fluxes induced by the currents i_{T1} and i_{T2} are reversed relative to those induced in the Stage 1.

4) Stage 4 (t_3–t_4): The magnetizing currents i_T1 and i_T2 are both negative. This current state is characterized by the indicated direction shown in Fig. 4(d). All magnetic fluxes induced by the currents i_{T1} and i_{T2} are reversed relative to those induced in the Stage 2.

Overall, a cancelled flux and an overlapped flux can be always observed in the each pair of diagonal legs, respectively. Since there is a 90° between the two excitation currents and 75% duty cycle, the triangular flux waveforms through each leg can be plotted in Fig. 5 where Φ_{S1}, Φ_{S2}, Φ_{S3}, and Φ_{S4} represent the overall flux through each secondary winding S_1, S_2, S_3, and S_4, respectively. This implies that square voltages with 50% duty cycle are produced in each secondary winding as symbols V_{S1}, V_{S2}, V_{S3}, and V_{S4} in Fig. 5.

For the different phase-shift angle between the two input power stages, the induced voltage waveforms on each secondary winding can be obtained by using the aforementioned analytical approach. As shown in Fig. 6, not only the shapes but also the amplitudes of the voltages are changed. The maximum output voltage for the dual-input isolated boost dc–dc converter is achieved in the cases of 0° and 180° phase shift. The minimum voltage is obtained in the case of 90° phase shift and the case of 45° phase shift causes an output voltage in between. In fact, this characteristic of the flux cancellation and adding in each pair of diagonal legs effectively changes turns ratio of the transformer. Accordingly, the output voltage can be controlled by the phase shift angle. The function of voltage gain in the converter cannot be simply described by the duty cycle and turns ratio since the phase shift angle has to be considered. The detailed function relationship of voltage gain specified to this converter will be analyzed in the future continued publication.

IV. Discussion of Advantages

A. Independent Operation

Since the two primary windings *AB* and *CD* are uncoupled, the two input power stages have the common ground and can be

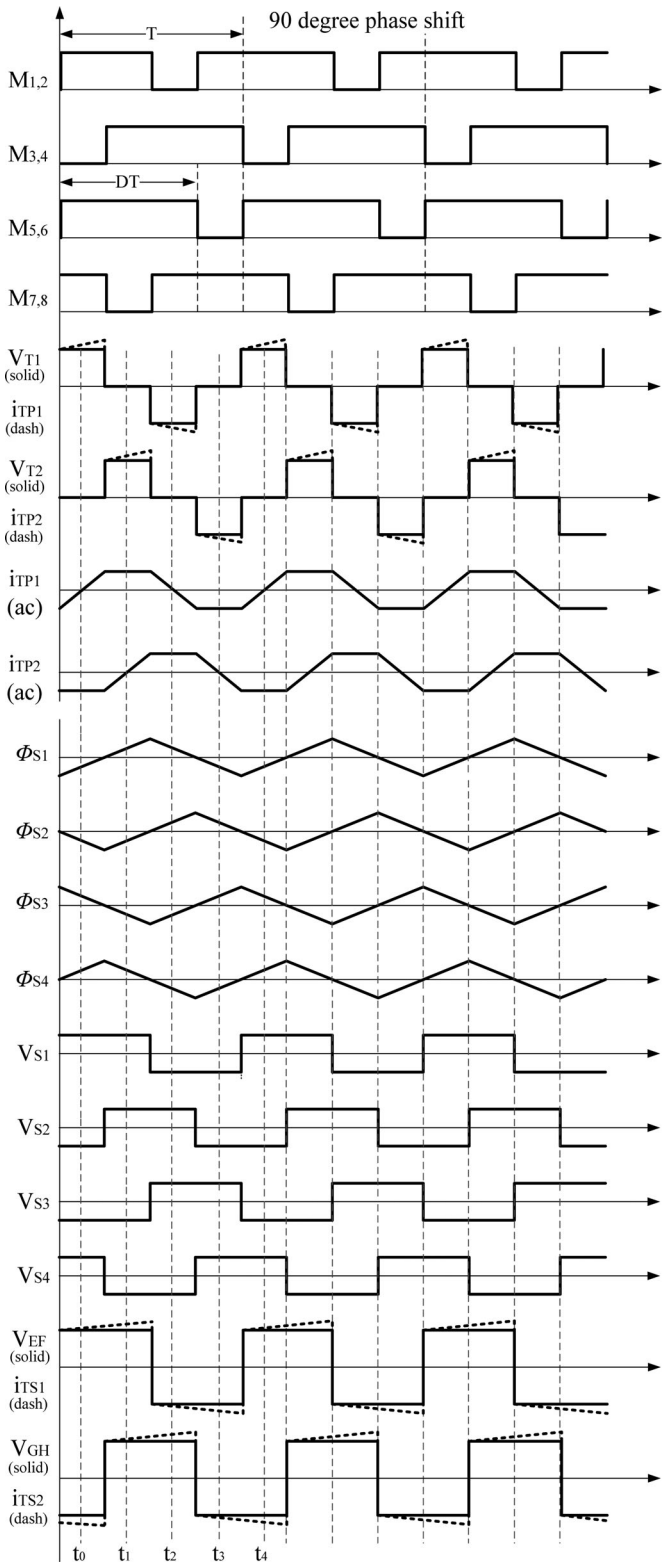

Fig. 5. Timing diagram and basic waveforms for the FQIT.

operated independently where the two input power sources are allowed to transfer the energy into the output simultaneously or at any time-multiplexing scheme. Meanwhile, the two power stages can be operated in different input voltage levels due to its independent operation. These advantages enable an operational reliability for the dual-input converter when any faults occur in one of the input power stages. Currently, these features cannot be implemented efficiently by using the traditional multiple-winding transformers with the flux additive. Furthermore, the FQIT can be applied in any type of topologies associated with multiple inputs. In addition, two discrete transformers with special-connected secondary are used to generate the complementary pulsewidth, and thus, solve the cross-regulation problem for the dual-output converters [12], [13]. The proposed FQIT may have a potential to overcome the cross-regulation problem without using complex control method for the dual-output converters.

B. Cost Effective, Low Size, and High Efficiency

Unlike a conventional multiple-input converter, the FQIT features minimized number of magnetic components without adding extra auxiliary circuit and switches. Hereby, this is a cost-effective way to implement the dual-input converter. Certainly, a lower size for the converter can be obtained as well. Furthermore, the flux cancellation occurring in the magnetic core may cause a lower core loss compared to the solutions with the discrete magnetic components, and thus a higher efficiency may be achieved.

C. Wide Range Input/Output Voltages

The output voltage is not only controlled by the duty cycle of PWM signal but also controlled by the phase-shift angle between the two input power stages. If a combination of duty cycle control and phase shift control is used in the dual-input converter, a wider range of input or output voltages, accordingly, can be achieved.

D. Waveforms Characteristics

50% duty cycle square waveforms without zero voltage platforms are induced on each secondary winding when the phase shift angle is 90°. Ideally, zero voltage ripple can be achieved in the load without any output capacitor. In addition, the current stress on the semiconductors of secondary side can be significantly reduced since the multilevel voltage waveforms are induced when the phase-shift angle is 45°. Moreover, since different output voltage waveforms are induced in the secondary windings as the different phase shift angle between the two input power stages, it may extensively derive some improved configurations for specific application.

However, the disadvantages of the FQIT are that the special core manufacture is needed and this winding structure may cause a higher leakage inductance than that of the traditional transformers.

V. Experimental Verification

In order to verify the correctness of the aforementioned analysis, a proof-concept experimental prototype with the proposed FQIT has been built. Fig. 7 shows the photo of the experimental prototype and the dimension of the employed FQIT and its subpicture are shown in Fig. 8. Mn-Zn ferrite is used

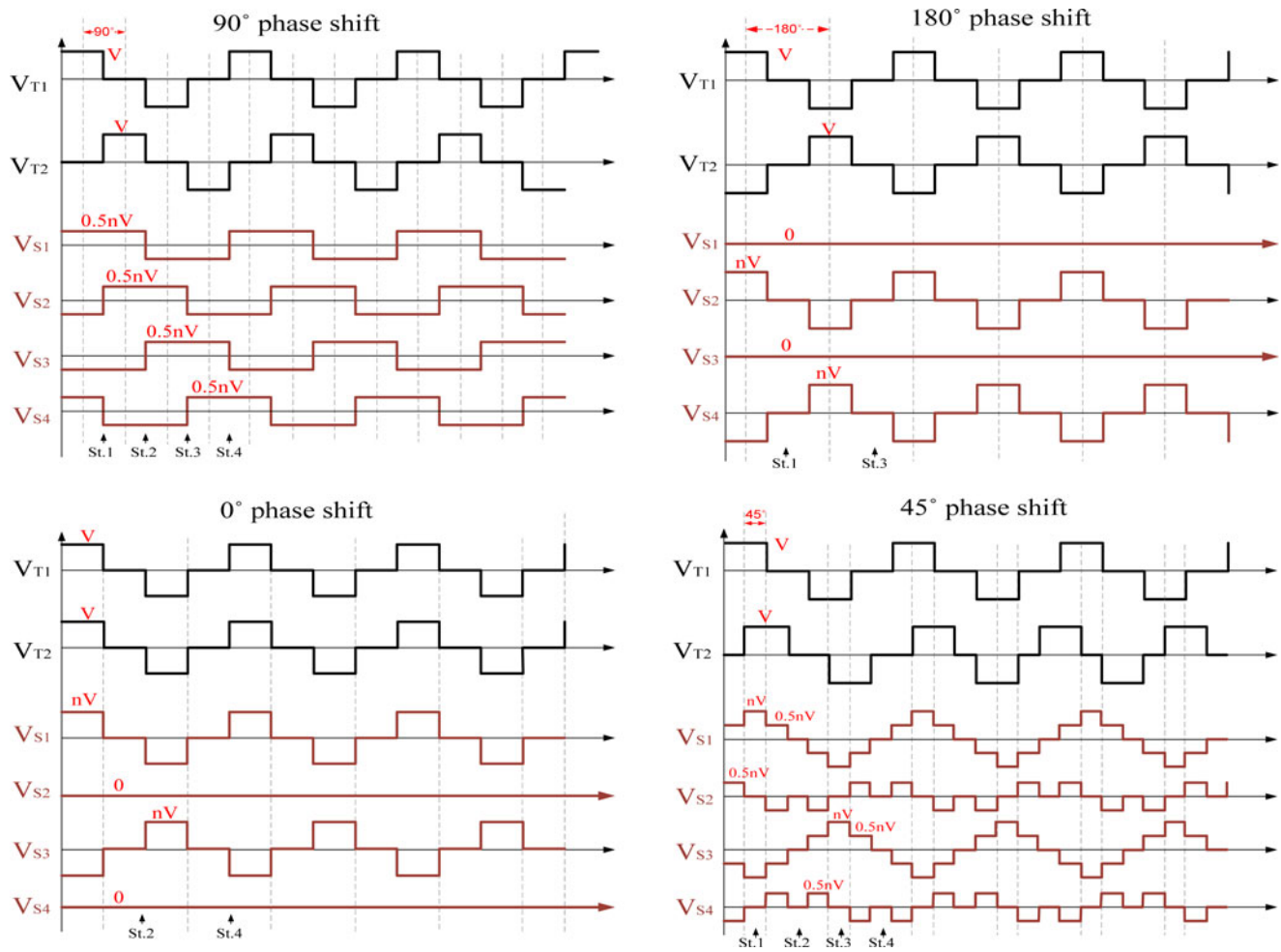

Fig. 6. Induced secondary voltages in each leg for different phase shift angles between two input power stages.

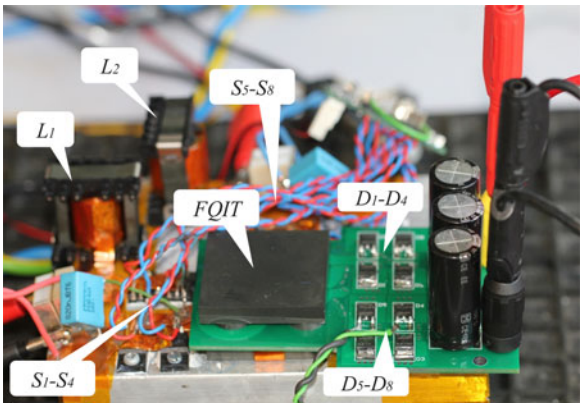

Fig. 7. Photo of experimental prototype with the FQIT.

as the material of magnetically permeable core. For simplification, one turn copper foil is used in the both primary sides and four turns are used in each secondary winding, which are implemented by the PCB winding. The switching frequency is operated at 100 kHz. The experimental results have excellently demonstrated that the two input power stages can be operated independently. Two terminal voltages of the primary windings, V_{AB} and V_{CD} (CH3&CH4), and two terminal voltages

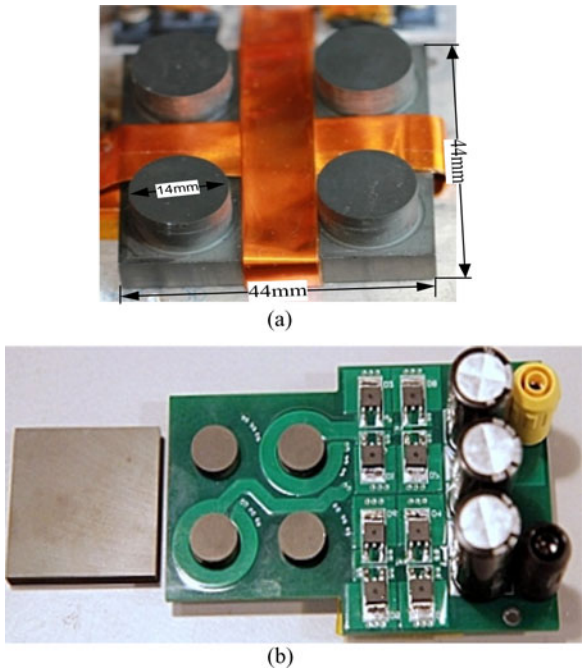

Fig. 8. Subpictures of the FQIT. (a) Primary windings. (b) Secondary windings.

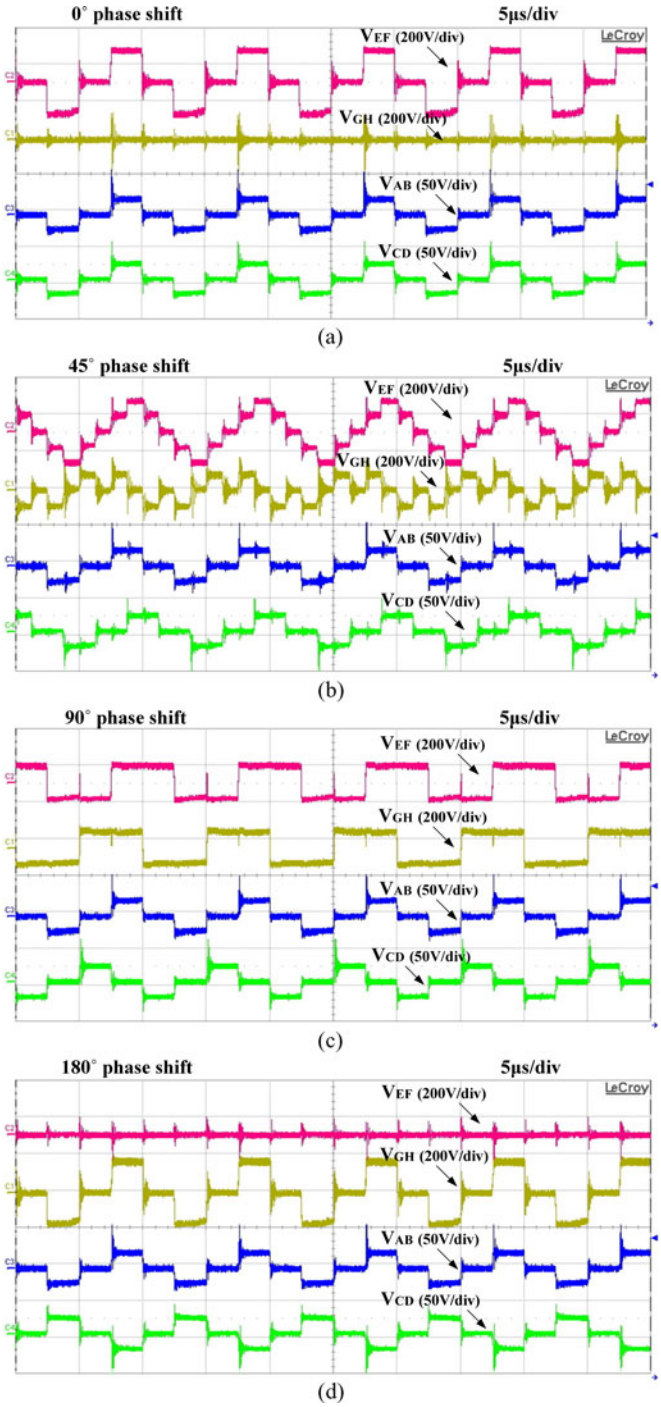

Fig. 9. Experimental waveforms for different phase shift angles.

of the series-secondary windings, V_{EF} and V_{GH} (CH1&CH2), are presented in Fig. 9. The two input dc voltages are both 12.5 V and the duty cycle are kept 75%. The output voltage can be adjusted by shifting the phase angle between the two power stages. Maximum 200-V output voltage is obtained when the phase angle is 0° or 180°. Minimum 100-V output voltage is obtained when the phase angle is 90°, and around 141-V output voltage is obtained when the phase angle is 45°. As seen in these plots, the experiment results have demonstrated the correctness of the analysis in Section III.

VI. Conclusion

This letter proposes a new concept for decoupling the primary windings in the integrated multiple-winding transformers based on 3-D space orthogonal flux decoupling. Only two orthogonal flux paths are utilized in the proposed FQIT and an applicable geometry of 3-D orthogonal flux decoupling can be found in [14]. The proposed FQIT allows the two input power stages to transfer the energy into the output simultaneously or at any time-multiplexing scheme. This enables a solution to the limitation of the traditional multiple-input converters. Many advantages of the FQIT such as cost effective, low size, and high efficiency have been discussed. In addition, wider range input/output voltages may be achieved since the phase shift between the two input power stages can be used to control the output voltage. This letter gives an applicable example of isolated boost dc–dc converter for the proposed FQIT. From the authors' points of view, the interesting waveforms induced on the secondary windings with the phase shift control may arouse some improved topologies development for specific application in future works.

References

[1] Y.-C. Liu and Y.-M. Chen, "A systematic approach to synthesizing multi-input dc–dc converters," *IEEE Trans. Power Electron.*, vol. 24, no. 1, pp. 116–127, Jan. 2009.

[2] K. Kobayashi, H. Matsuo, and Y. Sekine, "Novel solar-cell power supply system using a multiple-input DC–DC converter," *IEEE Trans. Ind. Electron.*, vol. 53, no. 1, pp. 281–286, Feb. 2006.

[3] H. Matsuo, T. Shigemizu, F. Kurokawa, and N. Watanabe, "Characteristics of the multiple-input dc-dc converter," *IEEE Trans. Ind. Electron.*, vol. 51, no. 3, pp. 625–631, Jun. 2004.

[4] K. P. Yalamanchili and M. Ferdowsi, "Review of multiple input dc–dc converters for electric and hybrid vehicles," in *Proc. IEEE Vehicle Power Propulsion Conf.*, Sep. 7–9, 2005, pp. 160–163.

[5] Y.-M. Chen, Y.-C. Liu, and F.-Y. Wu, "Multi-input dc/dc converter based on the multiwinding transformer for renewable energy applications," *IEEE Trans. Ind. Appl.*, vol. 38, no. 4, pp. 1096–1104, Jul. 2002.

[6] J. Ruan, F. Liu, X. Ruan, D. Yang, Y. Li, and K. Jin, "Isolated multiple-input dc/dc converter using alternative pulsating source as building cells," in *Proc. IEEE Int. Power Energy Conf.*, 2010, pp. 1463–1470.

[7] H.-J. Chiu, H.-M. Huang, L.-W. Lin, and M.-H. Tseng, "A multiple-input DC/DC converter for renewable energy systems," in *Proc. IEEE Int. Conf. Ind. Technol.*, Dec. 2005, pp. 1304–1308.

[8] Z. Ouyang, "Advances in planar and integrated magnetics," Ph.D. dissertation, Dept. Electr. Eng., Tech. Univ. Denmark, Kgs Lyngby, Denmark, 2011.

[9] S.S. Ochi and E. H. Wittenbreder, "Integrated multi-transformer," U.S. patent US20090230776A1, 2009.

[10] L. Yan, D. Qu, and L. B., "Integrated magnetic full wave converter with flexible output inductor," *IEEE Trans. Power Electron.*, vol. 18, no. 2, pp. 670–678, Mar. 2003.

[11] D. Cheng, L.-P. Wong, and Y.-S. Lee, "Design, modeling, and analysis of integrated magnetics for power converters," in *Proc. IEEE Power Electron. Spec. Conf.*, 2000, pp. 320–325.

[12] Y. Chen and Y. Kang, "A fully regulated dual-output DC–DC converter with special-connected two transformers (SCTTS) cell and complementary pulsewidth modulation–PFM (CPWM-PFM)," *IEEE Trans. Power Electron.*, vol. 25, no. 5, pp. 1296–1309, May 2010.

[13] Y. Chen and Y. Kang, "An improved full-bridge dual-output DC–DC converter based on the extended complementary pulsewidth modulation concept," *IEEE Trans. Power Electron.*, vol. 26, no. 11, pp. 3215–3229, Nov. 2011.

[14] Z. Ouyang, M. A. E. Andersen, and Z. Zhang, "Four quadrants transformers," U.S.&EU patent P1099US00, 2011 (pending).